

Supporting Information for
Efficient Polyalcohol Oxidation Electrocatalysts Enabled by PtM
(M=Fe, Co, Ni) Nanocubes Surrounded by (200) Crystal Facet

Tongxin Song, Fei Gao, Yangping Zhang, Chunyan Chen,

Cheng Wang, Shujin Li*, Hongyuan Shang, Yukou Du*

College of Chemistry, Chemical Engineering and Materials Science,

Soochow University, 199 Ren'ai Road, Suzhou 215123, P.R. China

**Corresponding author: E-mail: shujinli@suda.edu.cn (S. Li);*

duyk@suda.edu.cn (Y. Du).

Experimental section

Chemicals and Materials

Platinum (II) acetylacetonate ($\text{Pt}(\text{acac})_2$, reagent grade, 97%), Nickel (II) acetylacetonate ($\text{Ni}(\text{acac})_2$, 97%), Tungsten carbonyl ($\text{W}(\text{CO})_6$, reagent grade, 98%) Oleylamine (OAm, 80%) and 1-octadecylene (ODE, reagent grade, 90%) were purchased from Sigma-Aldrich. Cobalt acetylacetonate ($\text{Co}(\text{acac})_3$, 98%) was obtained from Aladdin Industrial Corporation. Iron acetylacetonate ($\text{Fe}(\text{acac})_2$, 97%) and citric acid (CA, Analytical Reagent, $\geq 99.5\%$) were acquired from Shanghai Macklin Biochemical Co., Ltd. Commercial Pt/C catalyst (20 wt%) was obtained from Shanghai Hesun Electric Co., Ltd. The average particle size was 2.8 nm. All chemicals were used directly without further purification.

Preparation of Pt_4M (M=Fe, Co, Ni) NCs

In the synthesis of Pt_4Ni NCs, $\text{Pt}(\text{acac})_2$ (10 mg), $\text{Ni}(\text{acac})_2$ (3.3 mg), $\text{W}(\text{CO})_6$ (5 mg) and CA (10 mg) were introduced into a glass vessel containing 3 mL of OAm, 2 mL of ODE and 0.1 mL of H_2O . After the mixture has undergone ultrasonic treatment for 1 h, the vessel was sealed and heated in oil bath at 160 °C and held for 5 h. Until cooling naturally, the product was centrifuged and washed with a mixture of cyclohexane and ethanol for three times. The Pt_4Fe NCs and Pt_4Co NCs were obtained by changing the 3.3 mg of $\text{Ni}(\text{acac})_2$ into 3.3 mg of $\text{Fe}(\text{acac})_2$ and 4.5 mg of $\text{Co}(\text{acac})_3$.

Physical characterizations

The structure of product was observed on HITACHI HT7700 transmission electron microscope (TEM). The high-resolution TEM, STEM-EDS mapping, high-angle annular dark field scanning transmission electron microscopy (HAADF-STEM), and the EDS line-scanning profile were performed on FEI Tecnai F20 TEM. The composition of element was detected on EVO 18 scanning electron microscope with energy-dispersive X-ray spectroscopy (SEM-EDS). The crystal property was obtained on X'Pert-Pro MPD diffractometer (PANalytical, Netherlands) with a $\text{Cu K}\alpha$ X-ray source ($\lambda=1.540598 \text{ \AA}$). And the X-ray photoelectron spectroscopy (XPS) was conducted on Thermo Scientific ESCALAB 250 XI X-ray photoelectron spectrometer.

Electrooxidation measurements

Before electrochemical tests, the collected Pt₄M NCs were supported on Vulcan XC72R carbon black, which was labeled as Pt₄M NCs/C, then were made into 0.4 mg_{Pt}mL⁻¹ catalysts suspension (containing 5% of Nafion). All measurements were performed on three-electrode CHI 660e electrochemical workstation. The glassy carbon electrode (GCE, diameter: 5 mm) covered with 5 μL of catalysts ink was used as the working electrode, the Pt wire as counter electrode and the saturated calomel electrode (SCE) as reference electrode. We scanned the cyclic voltammetry (CV) curves at a scanning rate of 0.05 V s⁻¹ in 0.1 M HClO₄ solution with the potential range of -0.3~0.9 V. Then we conducted the GOR in 1 M KOH + 1 M glycerol mixed solution and the EGOR in 1 M KOH + 1 M EG solution with the range of -0.9~0.3 V. The chronoamperometry (CA) test was performed in the same mixed solution at -0.25 V for 3600 s. And the continuous CVs was carried out for 250 cycles. Furthermore, the electrochemical impedance spectroscopy (EIS) was tested to evaluate the electronic conductivity.

Supplementary Figures and Tables

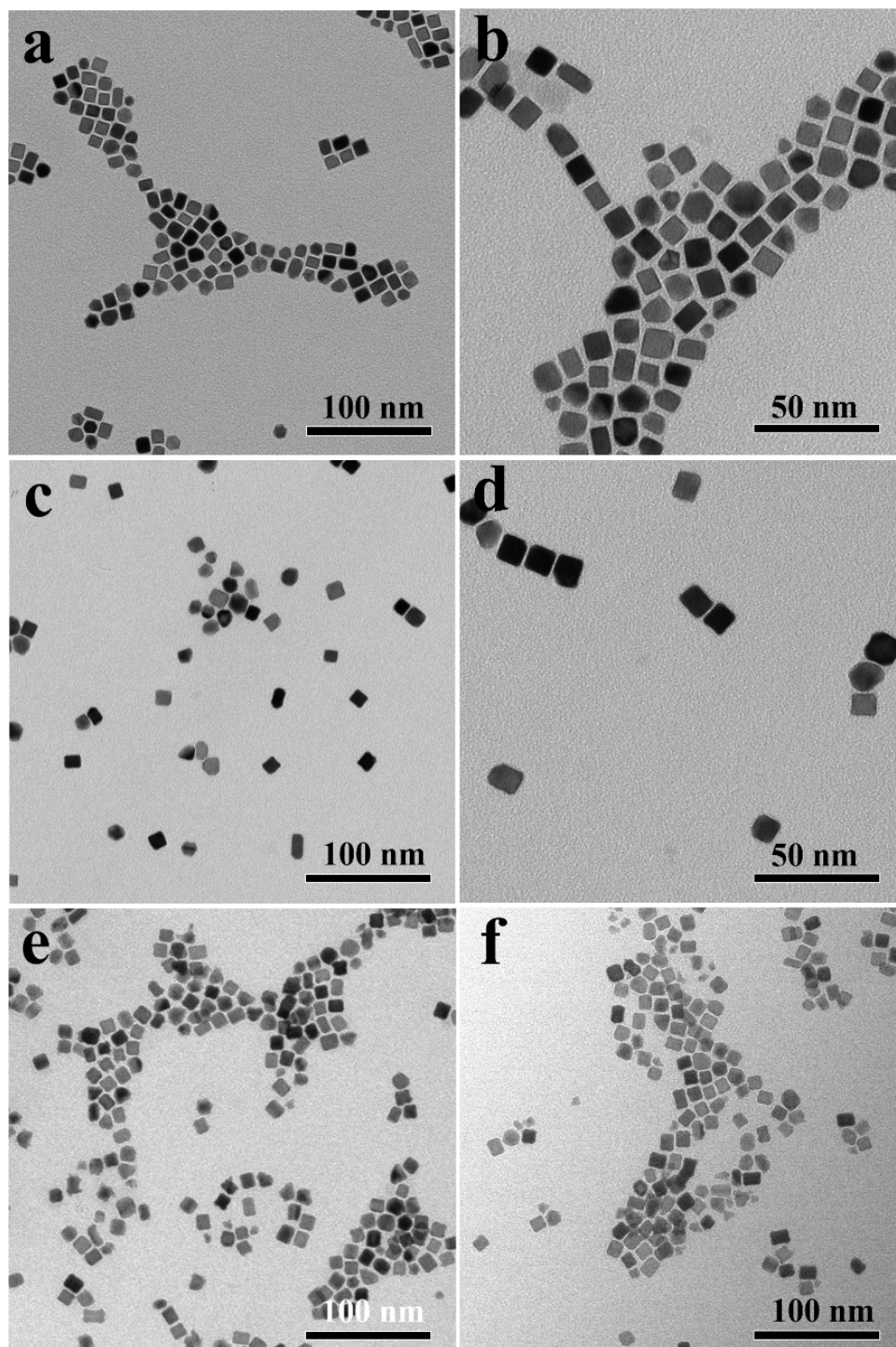


Fig. S1 Representative TEM images of the products with the same reaction conditions as that of Pt₄Ni NCs but changing the temperature: (a, b) 150 °C, (c, d) 170 °C, and (e, f) 180 °C.

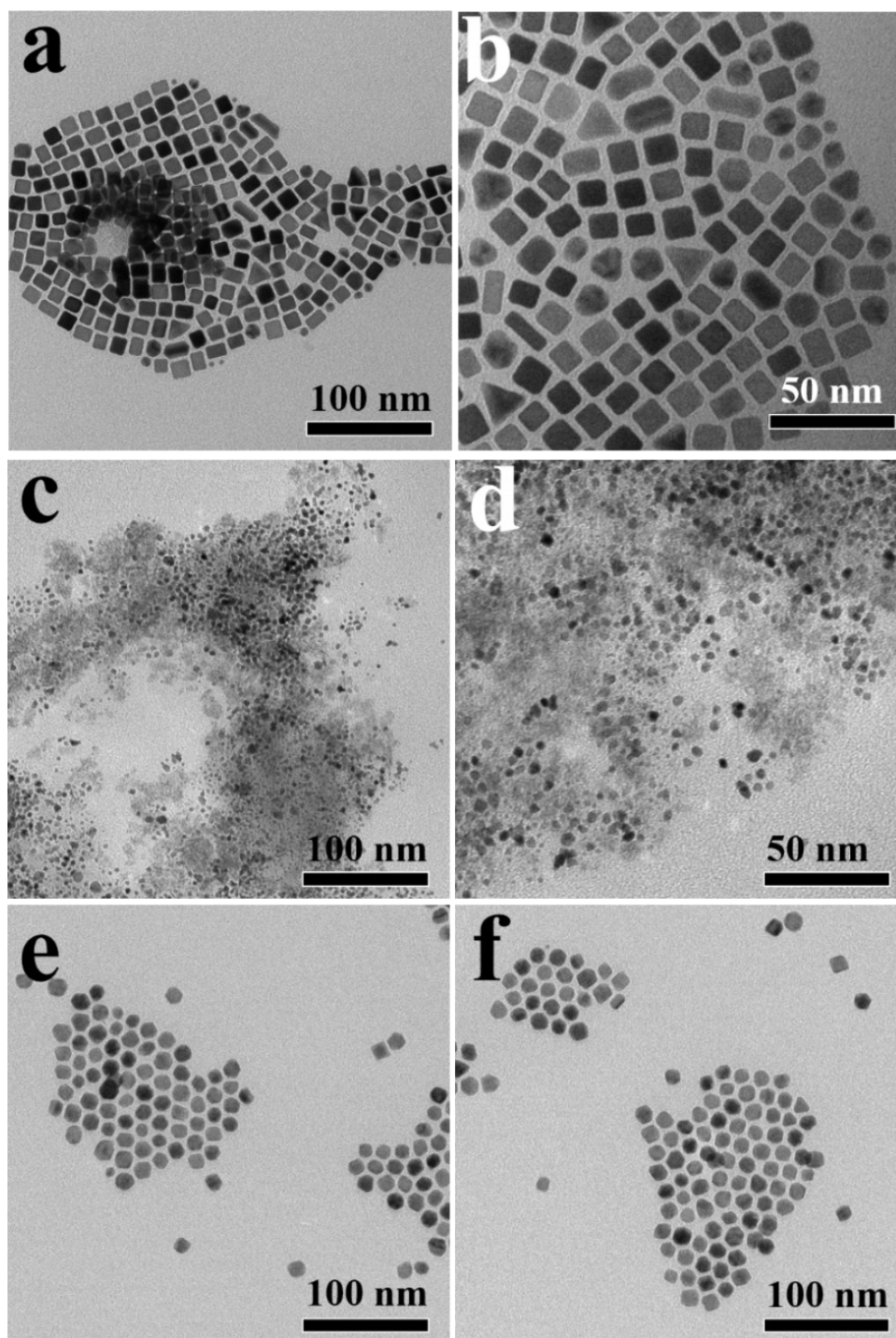


Fig. S2 Representative TEM images of the products with the same reaction conditions as that of Pt₄Ni NCs but changing the solvent: (a, b) 5 mL OAm, (c, d) 5 mL ODE, and (e, f) 4 mL OAm and 1 mL OA.

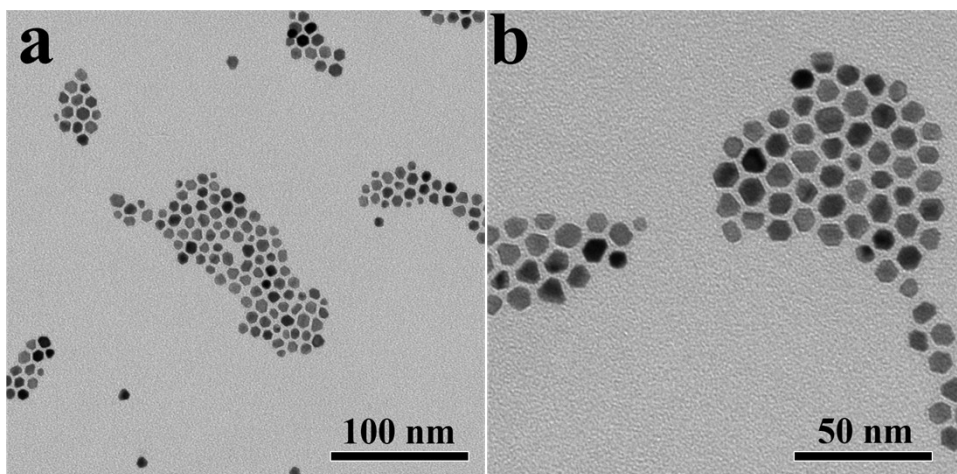


Fig. S3 Representative TEM images of the products with the same reaction conditions as that of Pt₄Ni NCs but without the water.

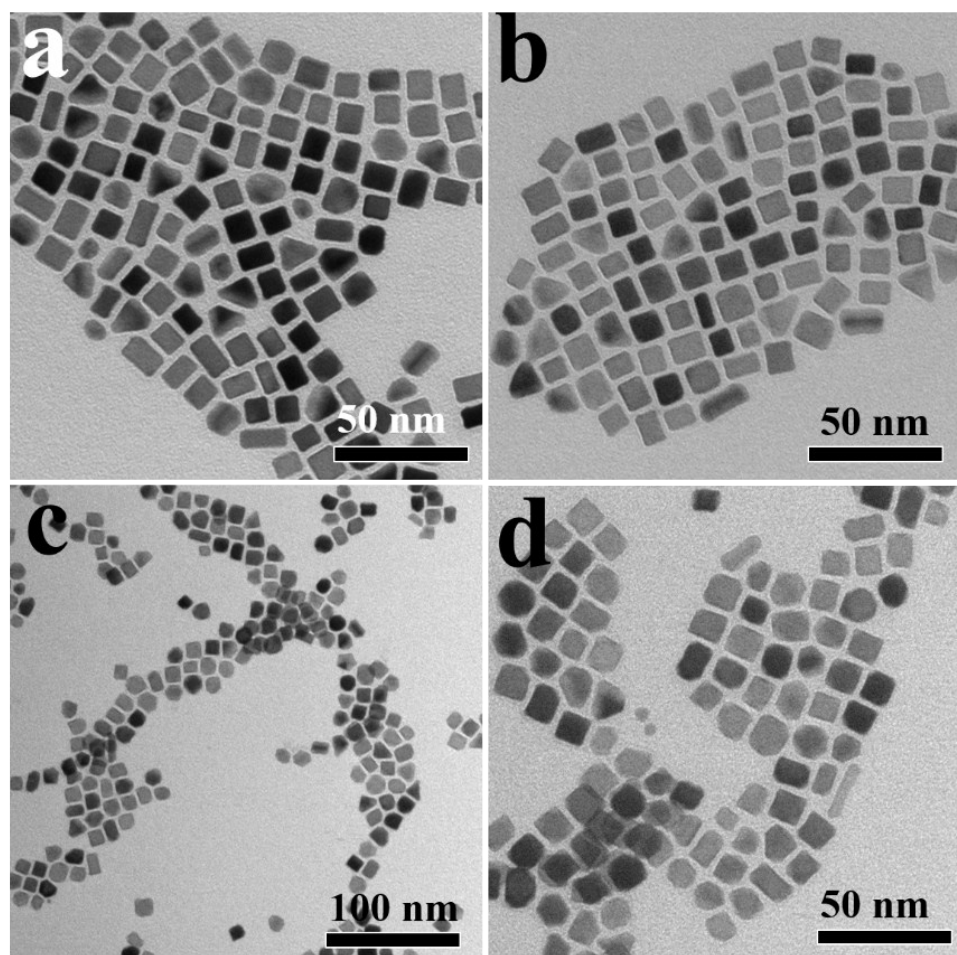


Fig. S4 Representative TEM images of the products with the same reaction conditions as that of Pt₄Ni NCs but changing the ratio of OAm to ODE: (a, b) 4 mL OAm and 1 mL ODE, and (c, d) 2 mL OAm and 3 mL ODE.

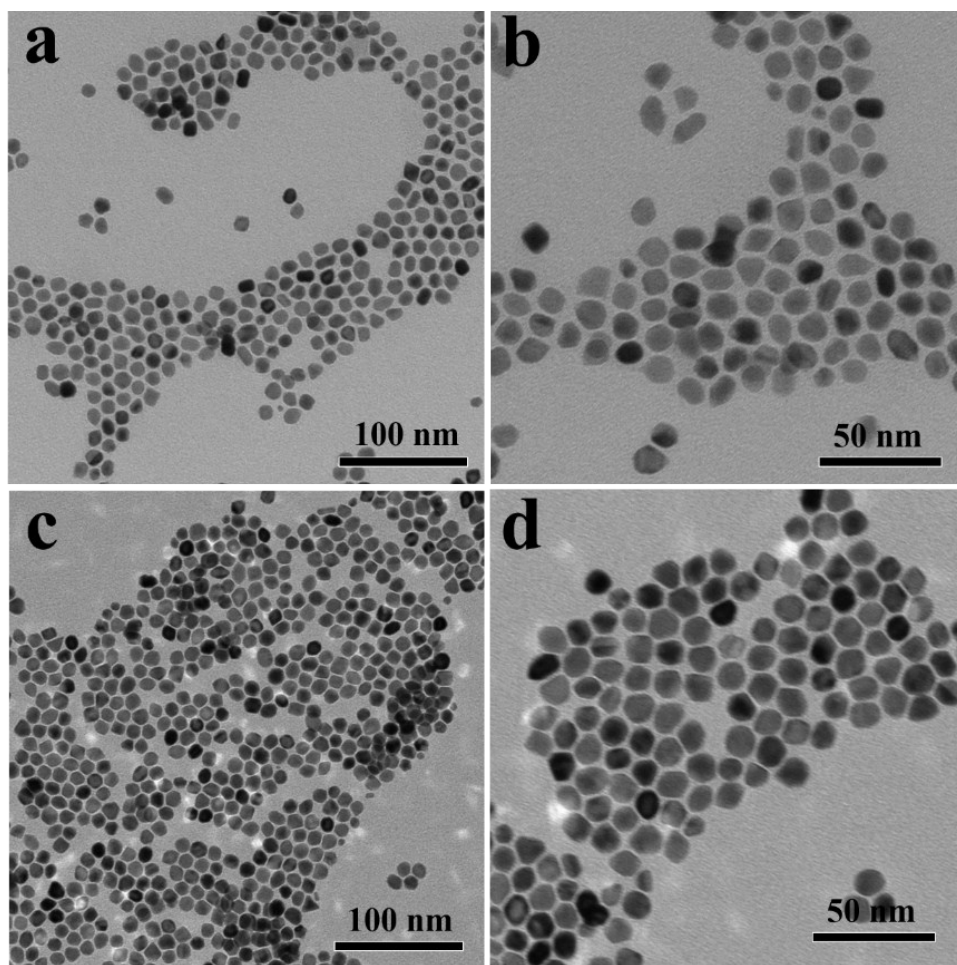


Fig. S5 Representative TEM images of the products with the same reaction conditions as that of Pt₄Ni NCs but varying amounts of W(CO)₆: (a, b) 10 mg, and (c, d) 20 mg. In the absence of W(CO)₆, the system has no products.

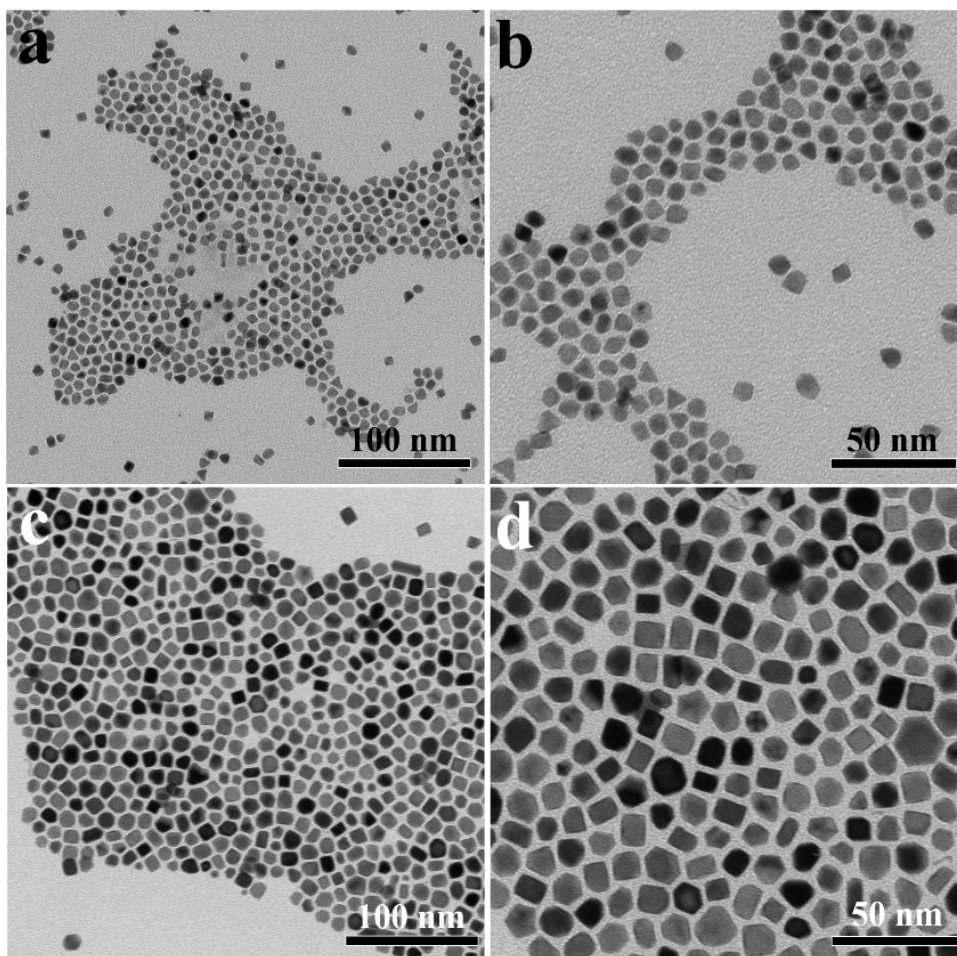


Fig. S6 Representative TEM images of the products with the same reaction conditions as that of Pt₄Ni NCs but varying amounts of CA: (a, b) 0 mg, and (c, d) 40 mg.

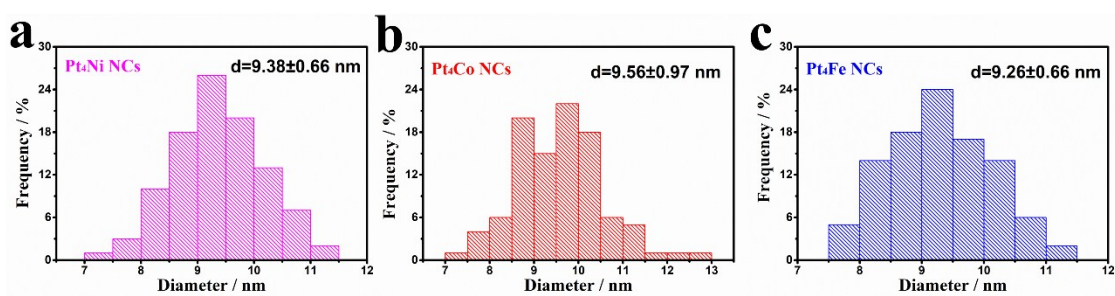


Fig. S7 The size distribution of (a) Pt₄Ni NCs, (b) Pt₄Co NCs, and (c) Pt₄Fe NCs.

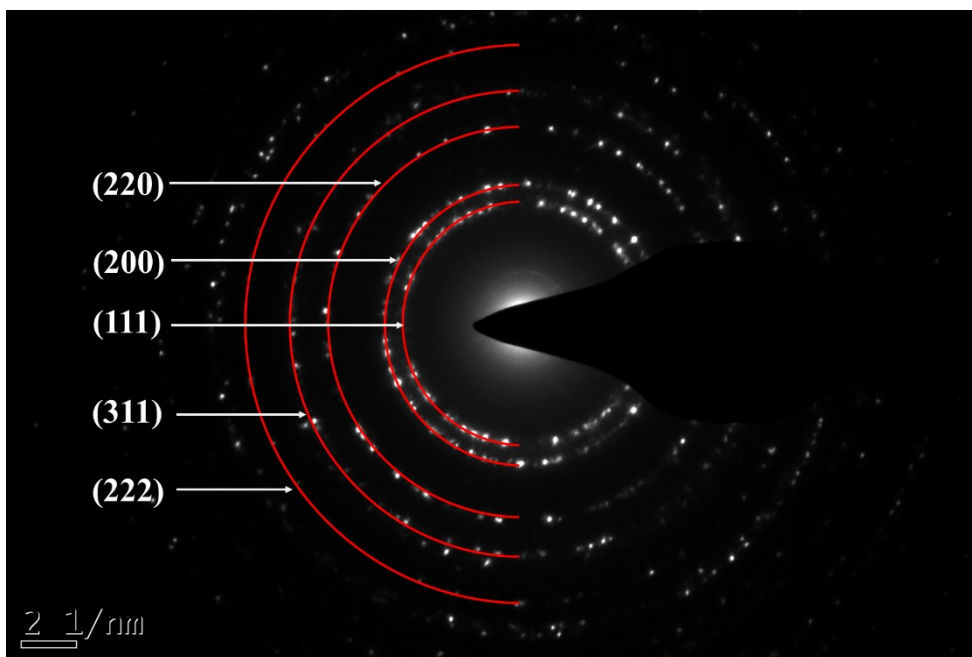


Fig. S8 The selected area electron diffraction pattern of the Pt₄Ni NCs.

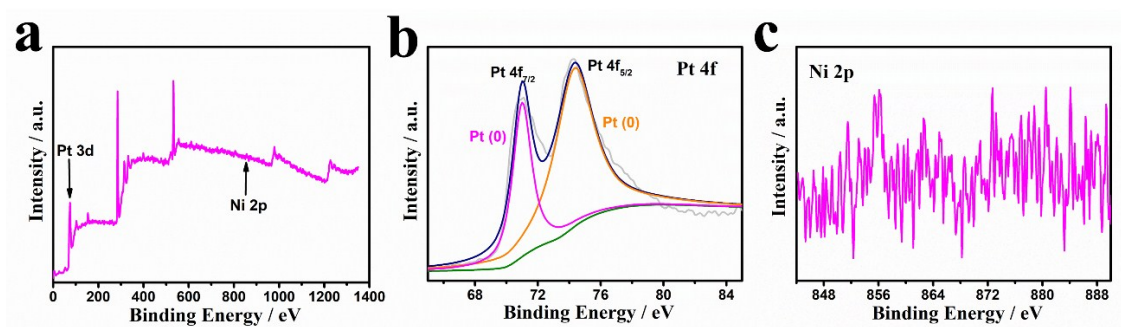


Fig. S9 The XPS analysis of (a) survey spectrum, (b) Pt 4f, and (c) Ni 2p in the Pt₄Ni NCs electrocatalysts.

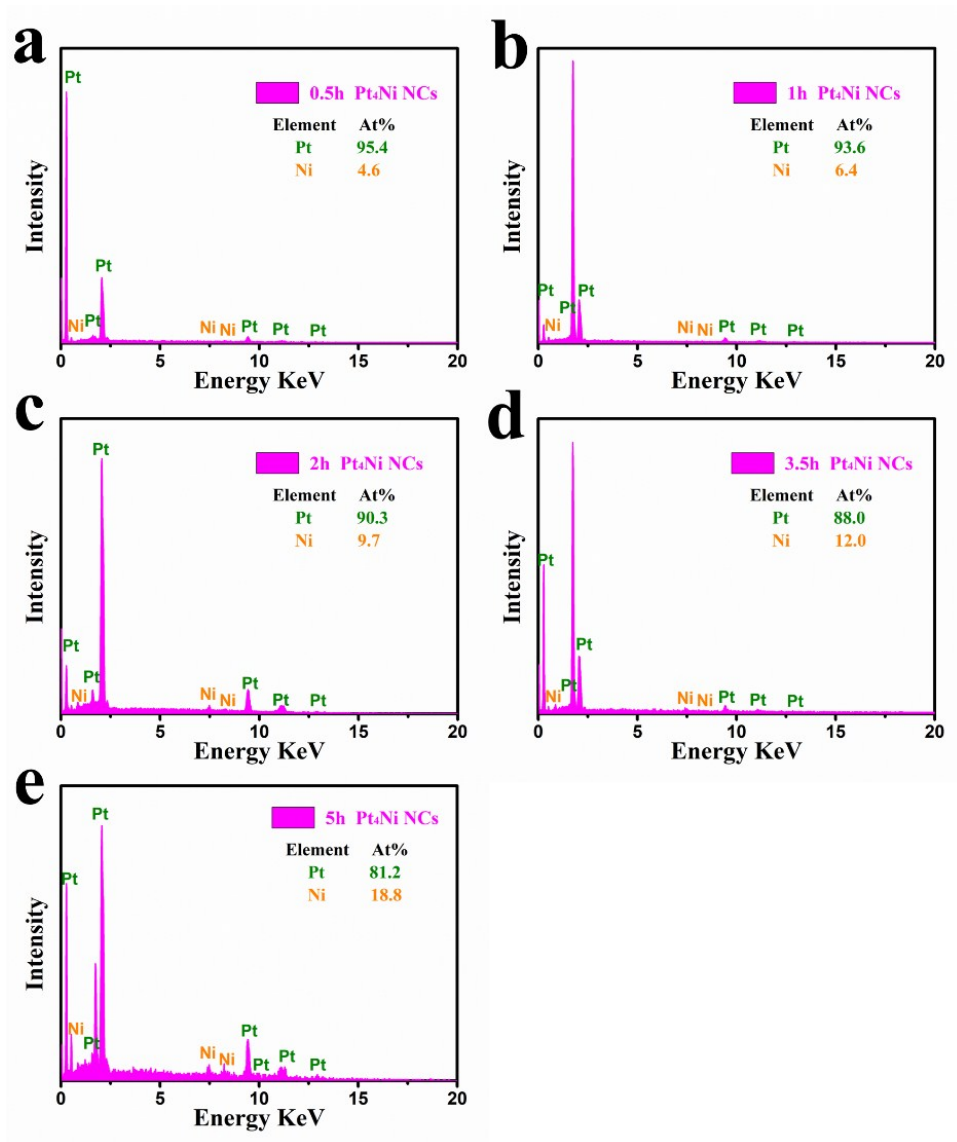


Fig. S10 The EDS spectrum of Pt₄Ni NCs intermediates obtained after the reaction have processed for (a) 30 min, (b) 1 h, (c) 2 h, (d) 3.5 h, and (e) 5h.

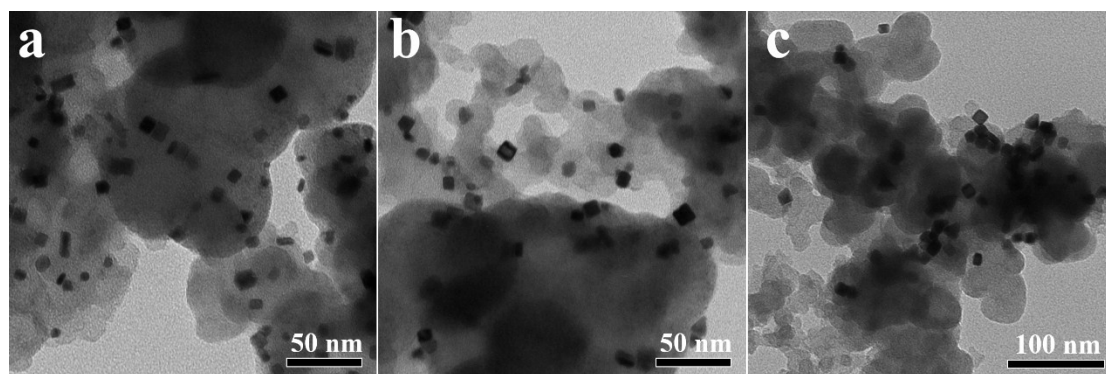


Fig. S11 The TEM images of (a) Pt₄Co NCs/C, (b) Pt₄Fe NCs/C, and (c) Pt₄Ni NCs/C.

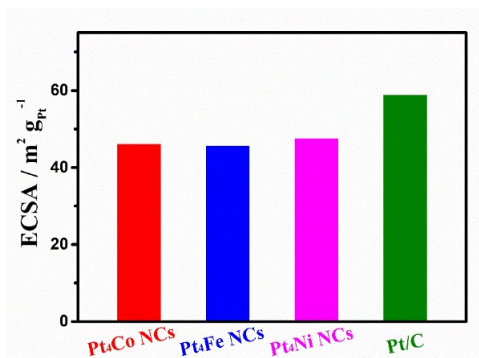


Fig. S12 The histograms of ECSA values of the four different electrocatalysts.

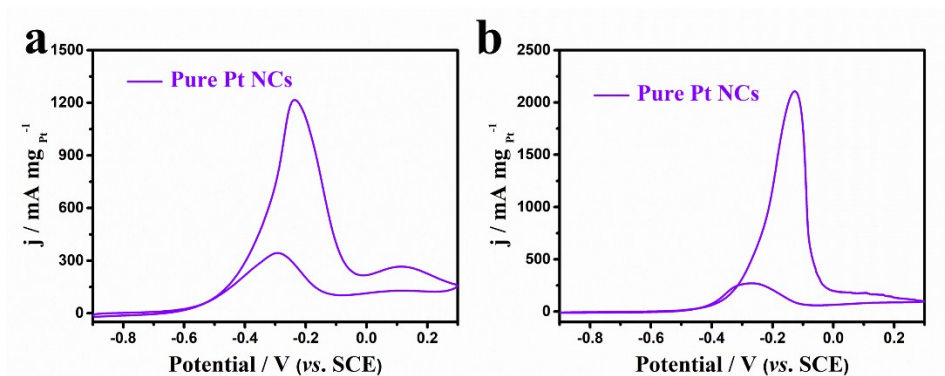


Fig. S13 The CV curves of pure Pt NCS towards (a) GOR in 1 M KOH+1 M glycerol at 0.05 V s^{-1} , and (b) EGOR in 1 M KOH+1 M EG at 0.05 V s^{-1} .

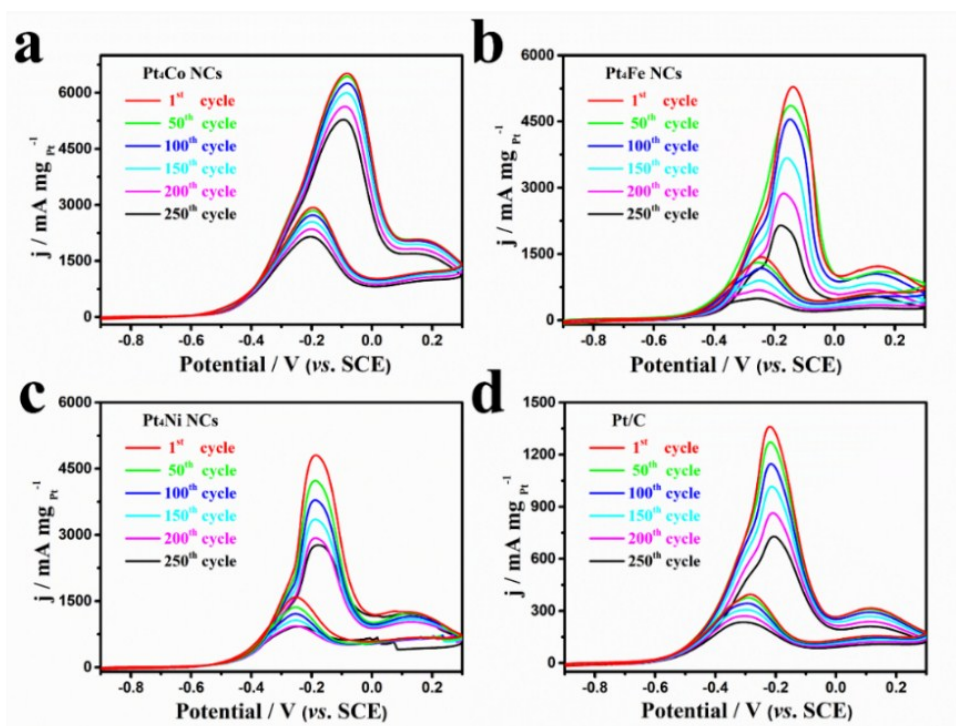


Fig. S14 The CV curves of (a) Pt₄Co NCS, (b) Pt₄Fe NCS, (c) Pt₄Ni NCS, and (d) commercial Pt/C catalysts towards GOR applying the successive CVs for 250 cycles.

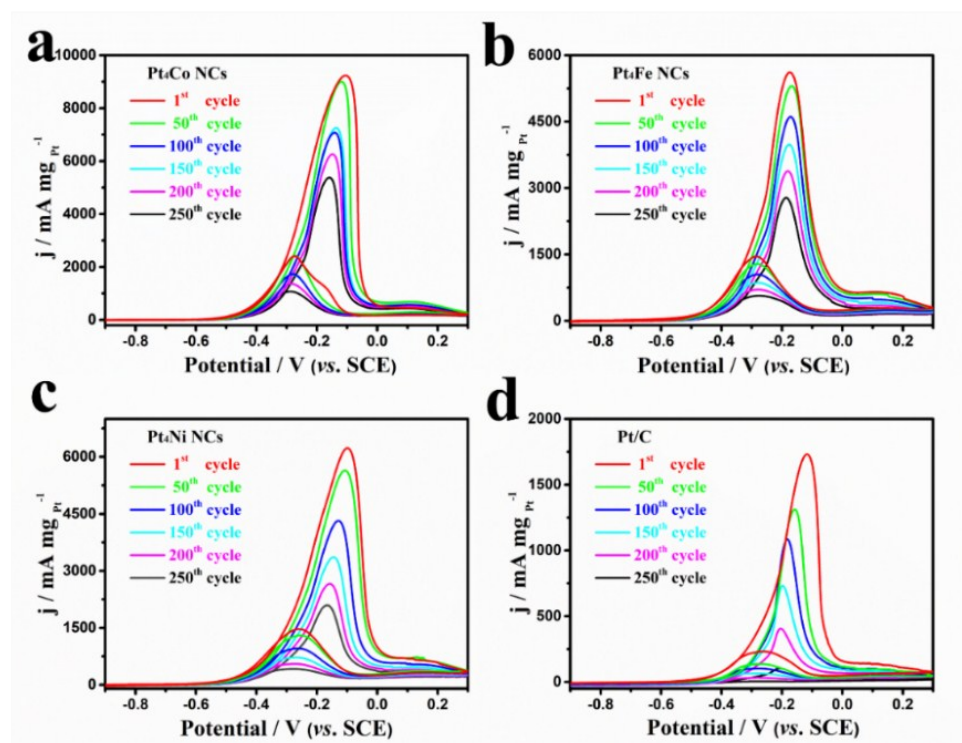


Fig. S15 The CV curves of (a) Pt₄Co NCs, (b) Pt₄Fe NCs, (c) Pt₄Ni NCs, and (d) commercial Pt/C catalysts towards EGOR applying the successive CVs for 250 cycles.

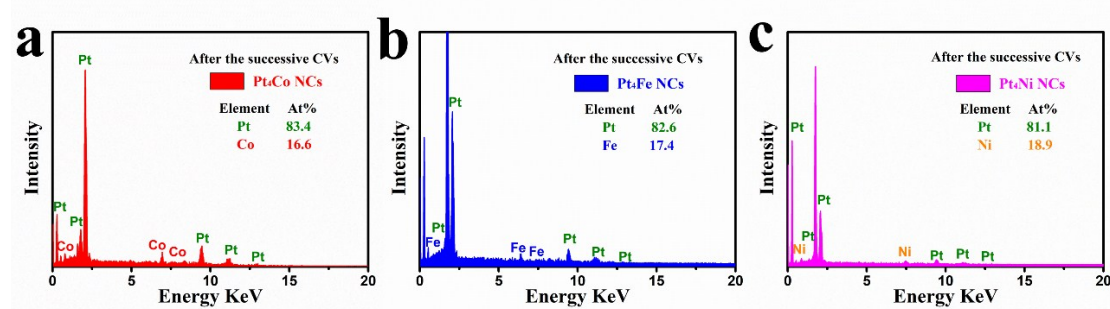


Fig. S16 EDS spectrum of (a) Pt₄Co NCs, (b) Pt₄Fe NCs, and (c) Pt₄Ni NCs catalysts after electrochemical durability test.

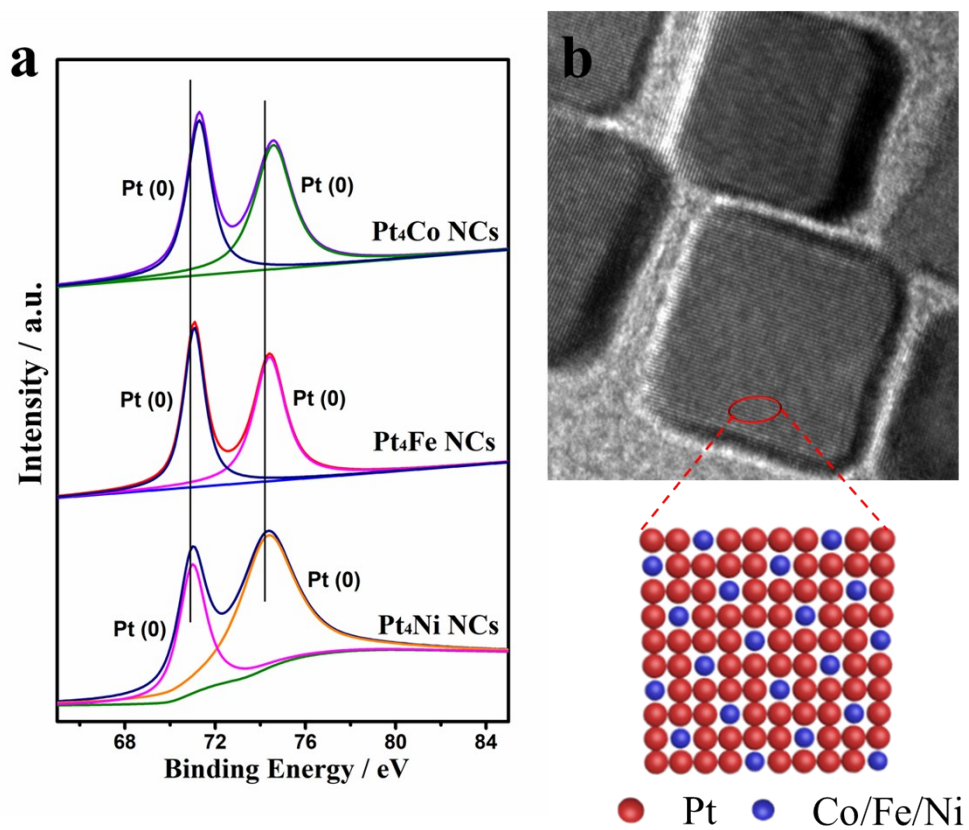


Fig. S17 (a) XPS spectra of Pt 4f in Pt₄M (Co, Fe, and Ni) NCs. (b) The schematic illustration of the improved electrocatalytic performance mechanisms of the Pt₄M (Co, Fe, and Ni) NCs.

Table S1 Other Pt-based electrocatalysts in different morphology for the glycerol electrochemical oxidation reaction in alkaline media.

Catalysts	Morphology	Electrolyte	Mass activity (mA mg ⁻¹)	Reference
Pt ₄ Co NCs	Nano-cubes	1 M KOH + 1 M glycerol	6320.0	This work
Pt ₃ Ni SNWs	Sinuous Nano- wires	1 M KOH + 1 M glycerol	4250.3	Nanoscale, 2019, 11 , 4831-4836
Pt ₈₉ Co NWs	Nano-wires	1 M KOH + 1 M glycerol	4573.0	J. Colloid Interf. Sci., 2019, 556 , 441-448
PtCo EDNC/C	Deeply Excavated Nano-cubes	1 M KOH + 0.1 M glycerol	~1200	Appl. Catal. B- Environ., 2019, 258 , 117951
PdPtCu NSs	Nano-sheets	0.1 M KOH + 0.1 M glycerol	~1400	Green Chem., 2019, 21 , 2367-2374
Pt ₃ Ni NRs	Nano-rods	1 M KOH + 1 M glycerol	4601.5	J. Power Sources, 2019, 425 , 179-185
Pt ₂ Au NWs	Nano-wires	1 M KOH + 0.1 M glycerol	3400	J. Electroanal. Chem., 2018, 811 , 37-45

Table S2 Other Pt-based electrocatalysts in different morphology for the ethylene glycol electrochemical oxidation reaction in alkaline media.

Catalysts	Morphology	Electrolyte	Mass activity (mA mg ⁻¹)	Reference
Pt ₄ Co NCs	Nano-cubes	1 M KOH + 1 M EG	9345.0	This work
Pt ₁ Cu ₁	Nano-spheres	1 M KOH + 1 M EG	2146.9	J. Colloid Interf. Sci., 2019, 551 , 81-88
Pt-Co EDNC/C	Deeply Excavated Nano-cubes	1 M KOH + 0.1 M EG	~2500	Appl. Catal., B: Environ., 2019, 258 , 117951
PtRu alloy	Nano-crystal	1 M KOH + 1 M EG	3052	Int. J. Hydrogen Energy, 2017, 42, 20720-20728